Optica Applicata, Vol. XLIX, No. 2, 2019
DOI: 10.5277/oa190202

Propagation of Gaussian Schell-model vortex beams in biological tissues

MEILING DUAN[1*], YANNAN TIAN[1], JINHONG LI[2]

[1]Department of Physics, North University of China, Taiyuan 030051, China

[2]Department of Physics, Taiyuan University of Science and Technology, Taiyuan 030024, China

[*]Corresponding author: meilingduan@nuc.edu.cn

The dependence of changes in the relative intensity and the spectral degree of coherence on the refractive-index C_n^2 of biological tissues, space correlation length σ_0 and wavelength λ of the Gaussian Schell-model (GSM) vortex and non-vortex beams in biological tissues has been studied. It is shown that the intensity distribution of GSM vortex beams passing through the biological tissues undergoes several stages. The bigger C_n^2 is, and the smaller σ_0 is, the quicker the intensity evolution is. The attenuation of intensity for GSM vortex beams is much slower than that of non-vortex beams, thus the beam quality of the former is better than the latter. When propagating through the biological tissue, the phase singularities of GSM vortex beams will appear. As the propagation distance increases, the position of the phase singularities will shift, and these points will disappear where the changes in the spectral degree of coherence of GSM vortex beams are consistent with those of GSM non-vortex beams. At the same propagation distance, the bigger C_n^2 is, and the smaller σ_0 and λ are, the shorter the distance between the phase singularities and the z axis is, when the propagation distance z is in the range of 0–50 μm.

Keywords: GSM vortex beams, intensity distribution, spectral degree of coherence, biological tissue.

1. Introduction

With the development of molecular biology and medicine, a great many of significant technologies have been developed, such as laser-induced breakdown spectroscopy, image reconstruction techniques, synchrotron radiation microanalysis, nanoscale secondary ion mass spectrometry and laser ablation inductively coupled plasma mass spectrometry [1, 2]. It is beneficial to understand the living tissues for providing a good insight into the physiological and pathological changes in animal tissues [3], develop tissue image technology and improve medical instruments, and so on [4–6]. On the other hand, because the optical properties of the tissue can be displayed by the optical

parameters of light beams propagating through biological tissues, for example, as a very important characteristic parameter of optical field, the change in the spectral degree of coherence is directly related to the changes in optical properties of medium and plays a great part in estimating the structure and function of the biological tissue. By means of measuring and analyzing a variety of mammalian tissues, in 1996 SCHMITT and KUMAR pointed that the spatial correlations in the refractive indices of different tissues have similar properties and reported the power spectrum model of mammalian tissue [7]. Recently, by virtue of the power spectrum, many studies have been devoted to the stochastic properties of electromagnetic beams propagating through biological tissues. ZHOU *et al*. researched the spectral shift of an electromagnetic Gaussian Schell-model (GSM) beam propagating through tissues and pointed out that the spectral shift from the blue-shift to the red-shift is closely dependent on the parameters of the tissue [8]. The change difference in statistical properties between the anisotropic and isotropic electromagnetic beams passing through the biological tissues has been compared and illustrated by numerical calculations [5]. The effect of the upper dermis of human on the state of polarization and coherence of a random electromagnetic beam also has been investigated [9–11]. The effects of partially coherent model and parameters of biological turbulence on the average intensity and spreading of the GSM, Laguerre Gaussian Schell model and Bessel Gaussian Schell model beams have been studied [12].

As far as we know, a great number of researches on propagation properties are concerned the non-vortex beams propagating through biological tissues [3–11], while those referred to the vortex beams propagating through biological tissues are scarce [13]. There, the influence of the topological charge on the normalized spectral density distribution and the spectral degree of coherence of stochastic electromagnetic vortex beams in biological tissue has been researched. We also have investigated the changes in the degree of polarization of random electromagnetic GSM vortex beams in biological tissues and found that on the same conditions the changes in generalized degree of polarization are more complicated than those in one point degree of polarization, and the changes in one point degree of polarization are more complex than those in the on-axis degree of polarization [14]. Given the significance of the visualization and quantification of morphologic features of living tissues to biomedical diagnosis [15], in this paper, we have studied the intensity and coherence properties of vortex beams propagating through biological tissues. The analytical propagation expressions of the cross-spectral density matrix elements for GSM vortex beams with topological charge $m = \pm 1$ through biological tissue are derived based on the extended Huygens–Fresnel principle. The dependence of the evolution of intensity distributions of GSM vortex beams propagating through biological tissues on the species of biological tissues, wavelength and space correlation length of beams, the distance between two field points and propagation distance has been discussed by numerical examples. As well as, the changes in the spectral degree of coherence also have been demonstrated in the similar means.

2. Theoretical model

The initial field of a Gaussian vortex beam at the plane $z = 0$ reads as [16, 17]

$$U(\mathbf{s}, z = 0) = [s_x + i\,\mathrm{sgn}(m)s_y]^{|m|} \exp\left(-\frac{s_x^2 + s_y^2}{w_0^2}\right) \tag{1}$$

where $\mathbf{s} \equiv (s_x, s_y)$ is the two-dimensional (2D) position vector, sgn specifies the sign function, m is the topological charge, w_0 denotes the waist width of the Gaussian part.

By introducing a Schell-correlator [18], the cross-spectral density function of the GSM vortex beams at the source plane $z = 0$ is expressed as

$$W^{(0)}(\mathbf{s}_1, \mathbf{s}_2, 0) = [s_{1x}s_{2x} + s_{1y}s_{2y} + i\,\mathrm{sgn}(m)s_{1x}s_{2y} - i\,\mathrm{sgn}(m)s_{2x}s_{1y}]^{|m|} \times \exp\left[-\frac{\mathbf{s}_1^2 + \mathbf{s}_2^2}{w_0^2}\right] \exp\left[-\frac{(\mathbf{s}_1 - \mathbf{s}_2)^2}{2\sigma_0^2}\right] \tag{2}$$

where $\mathbf{s}_i \equiv (s_{ix}, s_{iy})$ $(i = 1, 2)$ is the 2D position vector at the source plane $z = 0$, σ_0 denotes the spatial correlation length, and the topological charge m in following we take $m = \pm 1$. When $m = 0$, Eq. (2) will reduce to cross-spectral density of a GSM (non-vortex) beam, *i.e.*,

$$W^{(0)}(\mathbf{s}_1, \mathbf{s}_2, 0) = \exp\left[-\frac{\mathbf{s}_1^2 + \mathbf{s}_2^2}{w_0^2}\right] \exp\left[-\frac{(\mathbf{s}_1 - \mathbf{s}_2)^2}{2\sigma_0^2}\right] \tag{3}$$

According to the extended Huygens–Fresnel principle [19], the cross-spectral density function of GSM vortex beams propagating through biological tissues is expressed as

$$W(\boldsymbol{\rho}_1, \boldsymbol{\rho}_2, z) = \left(\frac{k}{2\pi z}\right)^2 \iint \mathrm{d}^2\mathbf{s}_1 \iint \mathrm{d}^2\mathbf{s}_2 W^{(0)}(\mathbf{s}_1, \mathbf{s}_2, 0) \times \exp\left\{-\frac{ik}{2z}\left[(\boldsymbol{\rho}_1 - \mathbf{s}_1)^2 - (\boldsymbol{\rho}_2 - \mathbf{s}_2)^2\right]\right\} \langle \exp[\psi^*(\boldsymbol{\rho}_1, \mathbf{s}_1) + \psi(\boldsymbol{\rho}_1, \mathbf{s}_1)]\rangle \tag{4}$$

where $\boldsymbol{\rho}_1$ and $\boldsymbol{\rho}_2$ are the position vectors at the z plane, z is propagation distance of a beam propagating in the biological tissue, k is the wave number related to the wavelength λ by $k = 2\pi/\lambda$, ψ denotes the random part of the complex phase of a spherical wave propagating through the biological tissue, and $\langle \cdot \rangle$ implies the averaging over the ensemble of the statistical realizations of the random medium and can be written as [20]

$$\langle \exp[\psi^*(\boldsymbol{\rho}_1, \mathbf{s}_1) + \psi(\boldsymbol{\rho}_2, \mathbf{s}_2)] \rangle$$

$$= \exp\left\{-4\pi^2 k^2 z \int_0^1 \mathrm{d}t \int_0^\infty \mathrm{d}\kappa\, \kappa\, \Phi(\kappa) \left[1 - J_0\left(\left|t(\boldsymbol{\rho}_1 - \boldsymbol{\rho}_2) + (1-t)(\mathbf{s}_1 - \mathbf{s}_2)\right|\kappa\right)\right]\right\} \tag{5}$$

where J_0 is the zero-order Bessel function, and $\Phi(\kappa)$ is known as the power spectrum of the index of refraction fluctuations. As for a variety of mammalian tissues such as human skin, the expression of $\Phi(\kappa)$ is written as [7]

$$\Phi(\kappa) = \frac{4\pi \langle \delta n^2 \rangle L_0^2 (\varsigma - 1)}{(1 + \kappa^2 L_0^2)^{\varsigma}} \tag{6}$$

where L_0 is the outer scale of the refractive-index size, the parameter ς is related to the fractal dimension of the tissue and is an indication of the classical turbulent behavior of tissue, and $\langle \delta n^2 \rangle$ is the ensemble averaged variance of the refractive index.

In Eq. (5), the expansion of $J_0(x)$ can be expressed as [5]

$$J_0(x) = \sum_0^m \frac{(-1)^m (x/2)^{2m}}{(m!)^2}, \qquad |x| < \infty \tag{7}$$

and we will take the front two items as its approximate expression, then the expression of $\langle \exp[\psi^*(\boldsymbol{\rho}_1, \mathbf{s}_1) + \psi(\boldsymbol{\rho}_2, \mathbf{s}_2)] \rangle$ can be rewritten as

$$\langle \exp[\psi^*(\boldsymbol{\rho}_1, \mathbf{s}_1) + \psi(\boldsymbol{\rho}_2, \mathbf{s}_2)] \rangle \cong -\frac{(\boldsymbol{\rho}_1 - \boldsymbol{\rho}_2)^2 + (\boldsymbol{\rho}_1 - \boldsymbol{\rho}_2)(\mathbf{s}_1 - \mathbf{s}_2) + (\mathbf{s}_1 - \mathbf{s}_2)^2}{\rho_0^2} \tag{8}$$

where

$$\rho_0^2(z) = \left(\frac{2\pi^3}{3} C_n^2 k^2 z\right)^{-1} \tag{9}$$

where C_n^2 is named as the structure constant of the refractive-index of the biological tissues, whose expression is

$$C_n^2 = \frac{\langle \delta n^2 \rangle}{L_0^2 (2 - \varsigma)} \tag{10}$$

To calculate conveniently, introducing two variables of integration

$$\mathbf{u} = \frac{\mathbf{s}_1 + \mathbf{s}_2}{2} \tag{11a}$$

$$\mathbf{v} = \mathbf{s}_1 - \mathbf{s}_2 \tag{11b}$$

Substituting Eqs. (2), (8) and (11) into Eq. (4), we obtain

$$W(\boldsymbol{\rho}_1, \boldsymbol{\rho}_2, z) = \left(\frac{k}{2\pi z}\right)^2 \exp\left[-\frac{ik}{2z}(\boldsymbol{\rho}_1^2 - \boldsymbol{\rho}_2^2)\right] \exp\left[-\frac{(\boldsymbol{\rho}_1 - \boldsymbol{\rho}_2)^2}{\boldsymbol{\rho}_0^2}\right] \exp\left[-\frac{(\boldsymbol{\rho}_1 - \boldsymbol{\rho}_2)\mathbf{v}}{\boldsymbol{\rho}_0^2}\right]$$
$$\times \iint \mathrm{d}^2\mathbf{u} \iint \mathrm{d}^2\mathbf{v} \left[\left(\mathbf{u}^2 - \frac{\mathbf{v}^2}{4}\right) \mp i(u_x v_y - u_y v_x)\right] \exp\left[-\frac{2}{w_0^2}\mathbf{u}^2\right] \exp\left[-\varepsilon \mathbf{v}^2\right]$$
$$\times \exp\left[-\frac{ik}{z}\mathbf{u}\mathbf{v}\right] \exp\left[\frac{ik}{z}(\boldsymbol{\rho}_1 - \boldsymbol{\rho}_2)\mathbf{u}\right] \exp\left[\frac{ik}{2z}(\boldsymbol{\rho}_1 + \boldsymbol{\rho}_2)\mathbf{v}\right] \tag{12}$$

where

$$\varepsilon = \frac{1}{2w_0^2} + \frac{1}{2\sigma_0^2} + \frac{1}{\rho_0^2} \tag{13}$$

and the symbol $\mp$ corresponds to $m = \pm 1$ at the source plane. Making use of the integral formula [21]

$$\int x^n \exp(-px^2 + 2qx)\mathrm{d}x = n! \exp\left(\frac{q^2}{p}\right) \sqrt{\frac{\pi}{p}} \left(\frac{q}{p}\right)^n \sum_{k=0}^{E\left[\frac{n}{2}\right]} \frac{1}{(n-2k)!k!} \left(\frac{p}{4q^2}\right)^k \tag{14}$$

the analytical expression of the cross-spectral density function of the GSM vortex beams propagating through the biological tissue can be obtained by tedious and straightforward integral calculations

$$W(\boldsymbol{\rho}_1, \boldsymbol{\rho}_2, z) = \exp\left[-\frac{ik}{2z}(\boldsymbol{\rho}_1^2 - \boldsymbol{\rho}_2^2)\right] \exp\left[-\frac{(\boldsymbol{\rho}_1 - \boldsymbol{\rho}_2)^2}{\boldsymbol{\rho}_0^2}\right] \left[\left(M_1 - \frac{M_2}{4}\right) \mp i(M_3 - M_4)\right] \tag{15}$$

where

$$M_1 = \frac{k^2 b_x b_y}{4z^2 \varepsilon c} \left(\frac{d_x^2 + d_y^2}{c^2} + \frac{1}{c}\right) \exp\left(\frac{d_x^2 + d_y^2}{c}\right) \tag{16}$$

$$M_2 = \frac{k^2 w_0^2}{8z^2 f} \left(\frac{g_x^2 + g_y^2}{f^2} + \frac{1}{f}\right) \exp\left(\frac{g_x^2 + g_y^2}{f}\right)$$
$$\times \exp\left[-\frac{k^2 w_0^2}{8z^2}(\rho_{1x} - \rho_{2x})^2 - \frac{k^2 w_0^2}{8z^2}(\rho_{1y} - \rho_{2y})^2\right] \tag{17}$$

$$M_3 = \frac{k^2 w_0 b_x d_x g_y}{4z^2\sqrt{2\varepsilon c^3 f^3}} \exp\left[-\frac{k^2 w_0^2}{8z^2}(\rho_{1y}-\rho_{2y})^2\right]\exp\left(\frac{d_x^2}{c}+\frac{g_y^2}{f}\right) \tag{18}$$

$$M_4 = \frac{k^2 w_0 b_y d_y g_x}{4z^2\sqrt{2\varepsilon c^3 f^3}} \exp\left[-\frac{k^2 w_0^2}{8z^2}(\rho_{1x}-\rho_{2x})^2\right]\exp\left(\frac{d_y^2}{c}+\frac{g_x^2}{f}\right) \tag{19}$$

$$b_x = \exp\left[-\frac{k^2}{16\varepsilon z^2}(\rho_{1x}+\rho_{2x})^2\right]\exp\left[\frac{1}{4\varepsilon\rho_0^2}(\rho_{1x}-\rho_{2x})^2\right] \times \exp\left[-\frac{ik}{4\varepsilon z\rho_0^2}(\rho_{1x}^2-\rho_{2x}^2)\right] \tag{20}$$

$$d_x = \left(\frac{ik}{2z}+\frac{ik}{4\varepsilon z\rho_0^2}\right)(\rho_{1x}-\rho_{2x})+\frac{k^2}{8\varepsilon z^2}(\rho_{1x}+\rho_{2x}) \tag{21}$$

$$g_x = \frac{ik}{4z}(\rho_{1x}+\rho_{2x})+\left(\frac{k^2 w_0^2}{8z^2}-\frac{1}{2\rho_0^2}\right)(\rho_{1x}-\rho_{2x}) \tag{22}$$

$$c = \frac{2}{w_0^2}+\frac{k^2}{4\varepsilon z^2} \tag{23}$$

$$f = \varepsilon+\frac{k^2 w_0^2}{8z^2} \tag{24}$$

According to the symmetry, b_y, d_y and g_y also can be obtained by the replacement of ρ_{1x} and ρ_{2x} in b_x, d_x and g_x with ρ_{1y} and ρ_{2y}, respectively.

For GSM vortex beams propagating through the biological tissue, the average intensity at the z plane can be obtained by substituting $\boldsymbol{\rho}_1 = \boldsymbol{\rho}_2 = \boldsymbol{\rho}$ in Eqs. (15)–(24):

$$I(\boldsymbol{\rho}, z) = W(\boldsymbol{\rho}, \boldsymbol{\rho}, z) \tag{25}$$

as well as the spectral degree of coherence in the propagation field at a pair of field points $(\boldsymbol{\rho}_1, z)$ and $(\boldsymbol{\rho}_2, z)$ has been given by [22]

$$\mu(\boldsymbol{\rho}_1, \boldsymbol{\rho}_2, z) = \frac{W(\boldsymbol{\rho}_1, \boldsymbol{\rho}_2, z)}{\sqrt{I(\boldsymbol{\rho}_1, z)}\sqrt{I(\boldsymbol{\rho}_2, z)}} \tag{26}$$

3. Evolution of the intensity distribution

We choose the upper dermis of human, deep dermis of mouse and intestinal epithelium of mouse as the specimens of numerical calculation. According to Eq. (10) and the data

in [7], the three refractive indices of the biological tissues mentioned above are obtained as $C_n^2 = 0.44 \times 10^{-3}$ μm^{-1}, $C_n^2 = 0.22 \times 10^{-3}$ μm^{-1}, and $C_n^2 = 0.06 \times 10^{-3}$ μm^{-1}, respectively.

The changes in relative intensity $I(\rho, z)/I(\rho, 0)_{\max}$ (the intensities ratio, at propagation distance z, $I(\rho, z)$ and the maximum value at the source plane $I(\rho, 0)_{\max}$) of a GSM vortex beam and a GSM non-vortex beam propagating through different biological tissues are shown in Fig. 1. The calculation parameters are $\lambda = 0.6328$ μm, $w_0 = 50$ μm, $\sigma_0 = 0.5$ μm and $C_n^2 = 0.44 \times 10^{-3}$ μm^{-1} in Fig. 1**a**, $C_n^2 = 0.22 \times 10^{-3}$ μm^{-1} in Fig. 1**b** and $C_n^2 = 0.06 \times 10^{-3}$ μm^{-1} in Fig. 1**c**. As can be seen from Figs. 1**a**–1**c**, at the initial plane the GSM vortex beam presents a dark core, whereas the GSM non-vortex beam presents a Gaussian profile. As the propagation distance z increases, the relative intensity values of both the GSM vortex beam and GSM non-vortex beam will decrease

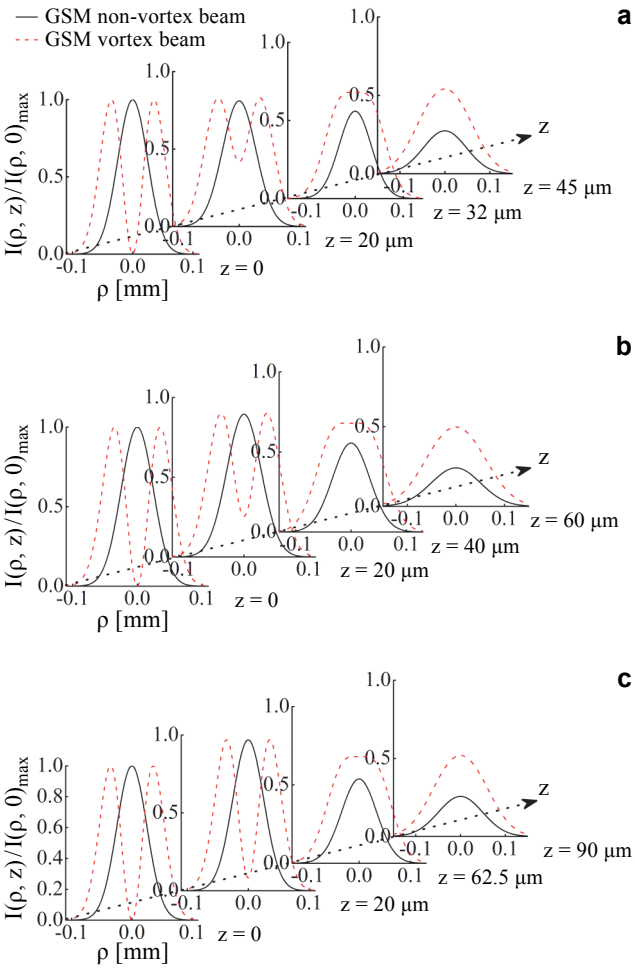

Fig. 1. Evolution of intensity distributions of a GSM vortex beam and a GSM non-vortex beam propagating through different biological tissues (see text for explanation).

gradually, and the intensity of beams become more and more weak. The propagation of GSM vortex beams through the different biological tissues undergoes several stages: a central dip, a flat-topped intensity profile, and a Gaussian profile. It can be attributed to the diffraction of the vortex beam during the propagation. A similar evolution behavior also can be present when a vortex beam propagates in atmospheric turbulence [23, 24] and oceanic turbulence [25, 26]. The random media, such as biological tissues, atmospheric turbulence and oceanic turbulence, will influence the evolution process of GSM vortex beams. A comparison among the Figs. 1**a**–1**c** suggests that at the same propagation distance the bigger structure constant C_n^2 corresponds to the smaller relative intensity, which means that the bigger C_n^2 is, the quicker the evolution of intensity distribution is. For example, the propagation distance of the flat-topped and Gaussian profile is z = 32 μm and 45 μm in Fig. 1**a**, z = 40 μm and z = 60 μm in Fig. 1**b**, and z = 62.5 μm and z = 90 μm in Fig. 1**c**, respectively. Therefore, the big C_n^2 will accelerate the evolution process of GSM vortex beams. Compared with the GSM non-vortex beams, the attenuation of intensity for GSM vortex beams is much slower, thus the beam quality of the GSM vortex beams is better than that of the GSM non-vortex beams.

Figure 2 shows the changes in relative intensity of GSM vortex beams propagating through upper dermis of human for different values of space correlation length σ_0, and the other calculation parameters the same as Fig. 1**a**. It can be found that at the source plane the intensity distribution is same for the GSM vortex beams with different σ_0, namely, the effect of space correlation length on the intensity distribution can be neglected. With increasing the propagation distance, the smaller σ_0 is, the quicker the evolution of intensity is, and the shorter the propagation distance of the flat-topped or Gaussian profile is. For example, at z = 20 μm the GSM vortex beam related to σ_0 = 0.05 μm has evolved into a Gaussian profile, whereas that related to σ_0 = 0.1 μm remains a flat -topped profile and that related to σ_0 = 0.5 μm keeps a central dip. As for the longer propagation distance (z = 45 μm), the bigger the space correlation length σ_0 is, the larger the maximum value of the relative intensity is, and the better the beam quality is.

Figure 3 depicts the changes in relative intensity of GSM vortex beams propagating through upper dermis of human for different wavelength λ; the calculation parameters

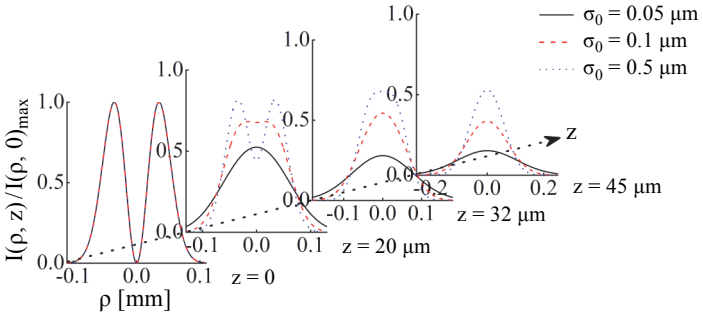

Fig. 2. Evolution of intensity distributions of a GSM vortex beam propagating through upper dermis of human for different values of space correlation length σ_0.

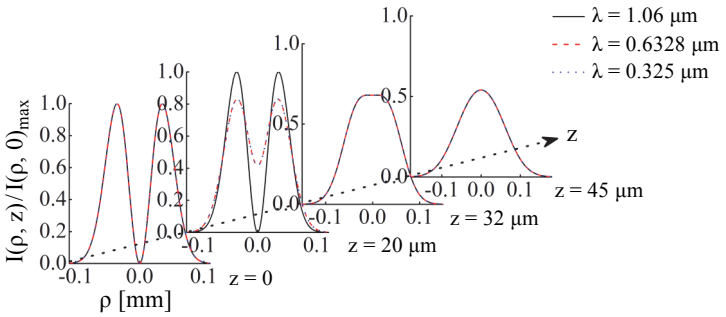

Fig. 3. Evolution of intensity distributions of a GSM vortex beam propagating through upper dermis of human for different wavelength λ.

are the same as Fig. 1**a**. We choose the wavelength parameters 0.325, 0.6328 and 1.06 μm, which represents the ultraviolet, the visible and the short infrared beam, respectively. It is illustrated that at the source plane ($z = 0$) the curves of intensity distribution are overlapped with each other, which indicates that the intensity distribution at the initial plane is independent of the wavelength of the GSM vortex beams. At the beginning of the propagation, for example $z = 20$ μm, the intensity distribution among the different GSM vortex beams displays different patterns. With increasing the propagation distance, the wavelength is negligible to the intensity evolution, for example at $z = 32$ μm and $z = 45$ μm, which implies that the difference of the wavelength λ of GSM vortex beams in intensity evolution is negligible when the propagation distance $z > 32$ μm.

4. Changes in spectral degree of coherence

The changes in spectral degree of coherence between two mixed points $\rho_1 = 0$ and $\rho_2 = \rho$ of a GSM vortex beam and that of a GSM non-vortex beam propagating through the different biological tissues are plotted in Fig. 4, and the calculation parameters are the same as Fig. 1. As shown in Fig. 4**a**, the spectral degree of coherence $\mu(0, \rho, z)$ of the GSM non-vortex beam decreases along with the propagation distance as the beam size expands during propagation. It also can be seen that the spectral degree of coherence of the GSM vortex beam has zero points, which implies the phase at these points is uncertain. Such points are therefore called phase singularities of the spectral degree of coherence [27]. One also find that the position of phase singularities of the GSM vortex beam will shift with increasing the propagation distance z, and these points will disappear, for example $z \geq 200$ μm, where the change of the spectral degree of coherence of the GSM vortex beam is consistent with that of the GSM non-vortex beam. This is attributed to the fact that the biological tissue is a random media, in which the wavefront of the GSM vortex beam will be distorted, and the destructive effect will be more and more strong with increasing propagation distance, so the wavefront will be broken as long as the propagation distance is long enough. The similar behavior

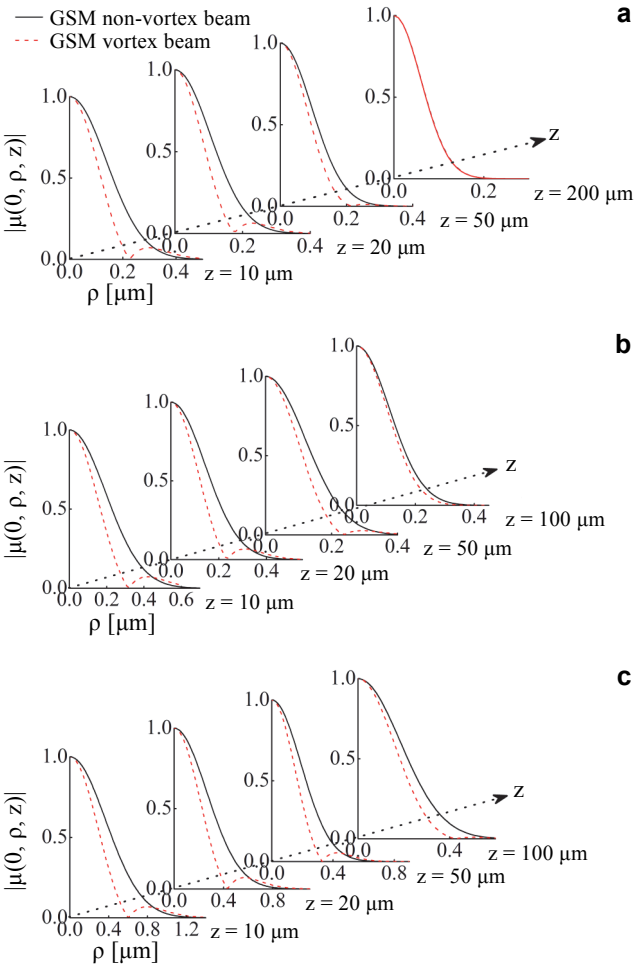

Fig. 4. Changes in the spectral degree of coherence for a GSM vortex beam and a GSM non-vortex beam propagating through different biological tissues (see text for explanation).

also can be presented when the vortex beam propagates in atmospheric turbulence [28]. From Figs. 4**a**–4**c** it can be observed that the bigger C_n^2 is, the shorter the distance between the phase singularities and z axis (point (0, 0)) is at the same propagation distance.

In Fig. 5 we depict the changes in the spectral degree of coherence of GSM vortex beams propagating through upper dermis of human for different space correlation length σ_0, and the calculation parameters being the same as for Fig. 1**a**. We can see that the influence of space correlation length σ_0 on the spectral degree of coherence is related to the propagation distance. When the propagation distance z is in the range of 0–50 μm, the GSM vortex beam with different σ_0 is characterized by various changes in the spectral degree of coherence. When the propagation distance $z > 100$ μm, the change curves approach to the consistent distribution, that is to say, the effect of the space correlation length on the spectral degree of coherence can be negligible.

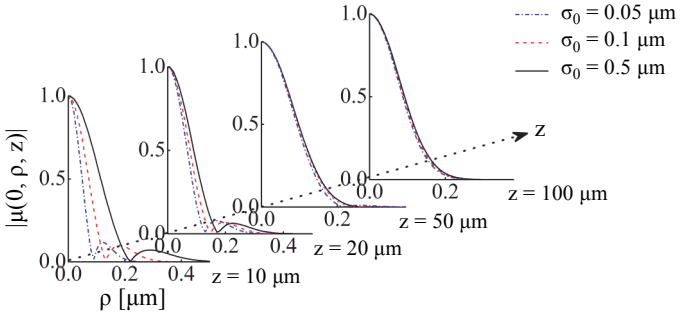

Fig. 5. Changes in the spectral degree of coherence for a GSM vortex beam and a GSM non-vortex beam propagating through upper dermis of human for different values of space correlation length σ_0.

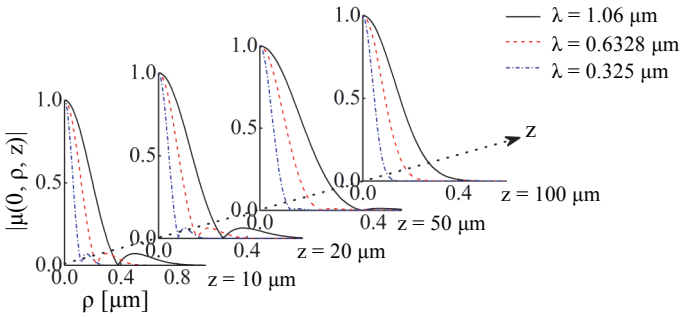

Fig. 6. Changes in the spectral degree of coherence for a GSM vortex beam and a GSM non-vortex beam propagating through upper dermis of human for different wavelength λ.

For different wavelength λ the changes in the spectral degree of coherence of GSM vortex beams propagating through upper dermis of human are discussed in Fig. 6; the calculation parameters are the same as Fig. 1**a**. We note that the GSM vortex beam with different wavelength λ experiences various change processes in the spectral degree of coherence, and the bigger λ is, the longer the distance between the position of phase singularities and point (0, 0) is.

5. Conclusions

Based on the extended Huygens–Fresnel principle, the analytical expressions of the cross-spectral density for GSM vortex beams propagating through biological tissues are derived, and used to study the dependence of the changes in both the relative intensity and the spectral degree of coherence of GSM vortex and non-vortex beams on the structure constant C_n^2, wavelength λ, space correlation length σ_0, the two points distance ρ and the propagation distance z. We find that the intensity distribution of GSM vortex beams passing through the biological tissues undergoes several stages: a central dip, a flat-topped intensity profile, and a Gaussian profile. The bigger C_n^2 is, the smaller σ_0 is, and the quicker the intensity evolution is. Besides, the smaller λ is,

the quicker the intensity evolution is when the propagation distance $0 < z < 20$ μm, whereas the influence of λ on the intensity evolution can be negligible when the propagation distance $z > 32$ μm. The phase singularities of GSM vortex beams will appear when propagating in the biological tissues, and these points will disappear as the propagation distance is increasing, for example at $z \geq 200$ μm, where the changes in the spectral degree of coherence of GSM vortex beams are consistent with those of GSM non-vortex beams. At the same propagation distance the bigger C_n^2 is, the smaller σ_0 and λ are, and the shorter the distance between the phase singularities and z axis is when the propagation distance $0 < z < 50$ μm. The results obtained in this paper may be applicable in the measurement of the intensity and spectral degree of coherence when a laser beam propagates through biological tissue and in the development of tissue imaging.

Acknowledgements – This work was supported by the Applied Basic Research Foundation of Shanxi Province, China (Grant No. 201701D121011), the Outstanding Young Scholars of Shanxi Province, China (Grant No. 201801D211006), and the Fund for Shanxi "1331 Project" key Innovative Research Team (1331KIRT).

References

[1] GIMENEZ Y., BUSSER B., TRICHARD F., KULESZA A., LAURENT J.M., ZAUN V., LUX F., BENOIT J.M., PANCZER G., DUGOURD P., TILLEMENT O., PELASCINI F., SANCEY L., MOTTO-ROS V., *3D imaging of nanoparticle distribution in biological tissue by laser-induced breakdown spectroscopy*, Scientific Reports **6**(7), 2016, p. 29936, DOI: 10.1038/srep29936.

[2] SCHOTT S., BERTOLOTTI J., LÉGER J.-F., BOURDIEU L., GIGAN S., *Characterization of the angular memory effect of scattered light in biological tissues*, Optics Express **23**(10), 2015, pp. 13505–13516, DOI: 10.1364/OE.23.013505.

[3] XINGYUAN LU, XINLEI ZHU, KUILONG WANG, CHENGLIANG ZHAO, YANGJIAN CAI, *Effects of biological tissues on the propagation properties of anomalous hollow beams*, Optik **127**(4), 2016, pp. 1842–1847, DOI: 10.1016/j.ijleo.2015.11.039.

[4] DE BOER J.F., MILNER T.E., VAN GEMERT M.J.C., NELSON J.S., *Two-dimensional birefringence imaging in biological tissue by polarization-sensitive optical coherence tomography*, Optics Letters **22**(12), 1997, pp. 934–936, DOI: 10.1364/OL.22.000934.

[5] XIAOYING LIU, DAOMU ZHAO, *The statistical properties of anisotropic electromagnetic beams passing through the biological tissues*, Optics Communications **285**(21–22), 2012, pp. 4152–4156, DOI: 10.1016/j.optcom.2012.06.033.

[6] DUAN MEILING, ZHANG CHAO, LI JINHONG, *Coherence and polarization properties of laser propagating through biological tissues*, Journal of Photochemistry and Photobiology B: Biology **172**, 2017, pp. 88–94, DOI: 10.1016/j.jphotobiol.2017.05.007.

[7] SCHMITT J.M., KUMAR G., *Turbulent nature of refractive-index variations in biological tissue*, Optics Letters **21**(16), 1996, pp. 1310–1312, DOI: 10.1364/OL.21.001310.

[8] FENG ZHOU, SHIJUN ZHU, YANGJIAN CAI, *Spectral shift of an electromagnetic Gaussian Schell-model beam propagating through tissue*, Journal of Modern Optics **58**(1), 2011, pp. 38–44, DOI: 10.1080/09500340.2010.543294.

[9] WANRONG GAO, *Changes of polarization of light beams on propagation through tissue*, Optics Communications **260**(2), 2006, pp. 749–754, DOI: 10.1016/j.optcom.2005.10.064.

[10] WANRONG GAO, KOROTKOVA O., *Changes in the state of polarization of a random electromagnetic beam propagating through tissue*, Optics Communications **270**(2), 2007, pp. 474–478, DOI: 10.1016/j.optcom.2006.09.061.

[11] WANRONG GAO, *Change of coherence of light produced by tissue turbulence*, Journal of Quantitative Spectroscopy and Radiative Transfer **131**, 2013, pp. 52–58, DOI: 10.1016/j.jqsrt.2013.03.006.

[12] YUQIAN WU, YIXIN ZHANG, QIU WANG, ZHENGDA HU, *Average intensity and spreading of partially coherent model beams propagating in a turbulent biological tissue*, Journal of Quantitative Spectroscopy and Radiative Transfer **184**, 2016, pp. 308–315, DOI: 10.1016/j.jqsrt.2016.08.001.

[13] MEILAN LUO, QI CHEN, LIMIN HUA, DAOMU ZHAO, *Propagation of stochastic electromagnetic vortex beams through the turbulent biological tissues*, Physics Letters A **378**(3), 2014, pp. 308–314, DOI: 10.1016/j.physleta.2013.11.022.

[14] YUNGUANG WU, MEILING DUAN, YIJUN LI, *Changes in the degree of polarization of random electromagnetic GSM vortex beams in biological tissues*, Optik **149**, 2017, pp. 95–103, DOI: 10.1016/j.ijleo.2017.09.020.

[15] WANRONG GAO, *Determination of spatial correlation functions of refractive index of living tissue*, Journal of Microscopy **245**(1), 2012, pp. 43–48, DOI: 10.1111/j.1365-2818.2011.03542.x.

[16] LI J., DING C., LÜ B., *Generalized Stokes parameters of random electromagnetic vortex beams propagating through atmospheric turbulence*, Applied Physics B: Lasers and Optics **103**(1), 2011, pp. 245–255, DOI: 10.1007/s00340-010-4289-y.

[17] JINHONG LI, JUN ZENG, MEILING DUAN, *Classification of coherent vortices creation and distance of topological charge conservation in non-Kolmogorov atmospheric turbulence*, Optics Express **23**(9), 2015, pp. 11556–11565, DOI: 10.1364/OE.23.011556.

[18] ZAHID M., ZUBAIRY M.S., *Directionality of partially coherent Bessel–Gauss beams*, Optics Communications **70**(5), 1989, pp. 361–364, DOI: 10.1016/0030-4018(89)90131-4.

[19] ANDREWS L.C., PHILLIPS R.L., *Laser Beam Propagation through Random Media*, Second Edition, SPIE Press, Bellingham 2005, DOI: 10.1117/3.626196.

[20] YURA H.T., *Mutual coherence function of a finite cross section optical beam propagating in a turbulent medium*, Applied Optics **11**(6), 1972, pp. 1399–1406, DOI: 10.1364/AO.11.001399.

[21] GRADSHTEYN I.S., RYZHIK I.M., *Table of Integrals, Series and Products*, Academic Press, New York, 2007.

[22] MANDEL L., WOLF E., *Optical Coherence and Quantum Optics*, Cambridge University Press, Cambridge, 1995.

[23] JINHONG LI, BAIDA LÜ, *Propagation of Gaussian Schell-model vortex beams through atmospheric turbulence and evolution of coherent vortices*, Journal of Optics A: Pure and Applied Optics **11**(4), 2009, article ID 045710, DOI: 10.1088/1464-4258/11/4/045710.

[24] JINHONG LI, BAIDA LÜ, *Composite coherence vortices in superimposed partially coherent vortex beams and their propagation through atmospheric turbulence*, Journal of Optics A: Pure and Applied Optics **11**(7), 2009, article ID 075401, DOI: 10.1088/1464-4258/11/7/075401.

[25] YONGPING HUANG, BIN ZHANG, ZENGHUI GAO, GUANGPU ZHAO, ZHICHUN DUA., *Evolution behavior of Gaussian Schell-model vortex beams propagating through oceanic turbulence*, Optics Express **22**(15), 2014, pp. 17723–17734, DOI: 10.1364/OE.22.017723.

[26] JIA XU, DAOMU ZHAO, *Propagation of a stochastic electromagnetic vortex beam in the oceanic turbulence*, Optics and Laser Technology **57**, 2014, pp. 189–193, DOI: 10.1016/j.optlastec.2013.10.019.

[27] WANG L., PONOMARENKO S.A., CHEN Z., *Spectral coherence anomalies*, Optics Letters **38**(14), 2013, pp. 2557–2559, DOI: 10.1364/OL.38.002557.

[28] GBUR G., TYSON R.K., *Vortex beam propagation through atmospheric turbulence and topological charge conservation*, Journal of the Optical Society of America A **25**(1), 2008, pp. 225–230, DOI: 10.1364/JOSAA.25.000225.

Received April 8, 2018
in revised form May 10, 2018